Journal of Electrotechnology, Electrical Engineering and Management (2023)
Clausius Scientific Press, Canada
DOI: 10.23977/jeeem.2023.060516
ISSN 2560-6697 Vol. 6 Num. 5

Research on optimized heliostat field based on dense circular arrangement

Sizhe Xie[1,*], Yao Li[1], Mingjie Yang[2]

[1]*Department of Electrical and Electronic Engineering, North China Electric Power University, Beijing, 100096, China*
[2]*School of Electrical Engineering, Northeast Electric Power University, Jilin, Jilin 132011, China*
[*]*Corresponding author: xsz_ncepu@163.com*

Keywords: Photovoltaic thermal power generation; Simulated annealing algorithm; Heliostat

Abstract: Solar energy is generally utilized in two ways. One is to utilize the photovoltaic effect to convert light energy into electrical energy; the other is to utilize sunlight radiation to convert light energy into heat energy. The second way is realized by the tower solar thermal power generation system in industry, and the main factor affecting the tower solar thermal power generation system is the fixed heliographic mirror field. In this paper, by establishing a physical model of the heliostat mirror field, a simulated annealing optimization algorithm is used to theoretically optimize the design of the existing heliostat mirror field, and ultimately an approximate dense circular arrangement of the mirror field is found, which results in the highest average annual power output per unit of mirror surface area. The final optimized fixed-sun mirror field arrangement in this paper will effectively improve the optical efficiency of the mirror field and contribute to the development of the photovoltaic industry.

1. Introduction

Tower solar thermal power generation systems use large-scale controllable heliostat mirrors to track and reflect sunlight and converge it onto the collector located at the top of the absorption tower. As the key part of the tower solar thermal power station, the array arrangement and efficiency of the heliostat mirror field is an important factor in determining the collector efficiency. Therefore, the optimal design of heliostat mirrors and the optimal arrangement of the mirror field are of great significance for the efficient utilization of solar energy and the improvement of the efficiency of the power station. The traditional fixed-sun mirror field arrangement often adopts a circular arrangement, this arrangement does not maximize the land resources, that is, the arrangement of fixed-sun mirrors doesn't reach the most intensive arrangement state, and the construction process lacks a complete theoretical model for guidance.

In this paper, the latitude and longitude of the heliostat mirror field, the variation of solar rays, the arrangement of the mirror field, and the size of the collector tower are considered comprehensively to establish a mathematical model of the heliostat mirror field. In this related paper[1], a mathematical model was proposed for the analysis of the optical efficiency of the solar tower power plant. Detailed optical losses are mainly losses by blockage, shading, spillage, and atmospheric mitigation. And in

this related paper[2], the mathematical model of the integrated drive system is developed, including the solar, tower, and heliostat models. Then the optimal arrangement of the mirror field is calculated by using modern optimization algorithms such as simulated annealing algorithm, particle swarm algorithm, genetic algorithm, and so on.

2. Calculation method of annual output power of heliostat field

Firstly, the variation of the sun's rays is described. The established mathematical model assumes that the sun's rays are parallel beams, which are only determined by the sun's altitude and azimuth angles. Due to the rotation of the sun and the rotation of the earth, the azimuth angle of the sun and the altitude angle of the sun are different at different times, and the control system controls the normal direction of the heliostat according to the real-time position of the sun to improve the utilization of light. To simplify the model calculation, the time points are taken as 9:00, 10:30, 12:00, 13:30, and 15:00 local time on the 21st day of each month.

Secondly, the way the mirror field is arranged determines the optical efficiency of the mirror field[3-5]. The optical efficiency η of the mirror field is calculated as follows:

$$\eta = \eta_{sb}\eta_{cos}\eta_{at}\eta_{trunc}\eta_{ref} \tag{1}$$

Therefore, the optical efficiency is determined by five sub-efficiencies, the shadow masking efficiency η_{sb}, the cosine efficiency η_{cos}, the atmospheric transmission efficiency η_{at}, the truncation efficiency η_{trunc}, and the specular reflection efficiency η_{ref}. The average annual output power E_{year} of a fixed-sun mirror field can be calculated by the following formula:

$$E_{year} = DNI * \sum_i^n A_i\eta_i \tag{2}$$

It can be seen that the annual average output power is mainly determined by four factors such as the normal direct radiation irradiance DNI, the total number of heliostats n, the light-gathering area A_i of the heliostat and its optical efficiency η_i.

The normal direct radiation irradiance DNI can be calculated by the following equation:

$$\begin{cases} DNI = G_0(a + be^{-\frac{c}{sin\alpha_s}}) \\ a = 0.4237 - 0.00821(6 - H)^2 \\ b = 0.5055 + 0.00595(6.5 - H)^2 \\ c = 0.2711 + 0.01858(2 - H)^2 \end{cases} \tag{3}$$

a, b, c are constants and are only related to the altitude $H(Km)$ of the heliostat mirror field. So the value of DNI is only related to the sun's altitude angle α_s in the case of a fixed mirror field location.

3. The model of sun ray

The sun's rays can be considered as parallel beams for a heliostat field. The position of the sun is only determined by the time, so for a heliostat mirror at the same time and in the same place, the vector of incident light from the sun is the same. The incident light reflected by the heliostat needs to be directed to the heat absorber, so the coordinates of the mirror and the coordinates of the heat absorbing tower are known to determine the vector of the reflected light.

First, determine the sun's altitude angle and azimuth angle, following that is to find the sun's altitude angle α_s and azimuth angle γ_s, the formula is as follows:

$$\begin{cases} sin\alpha_s = cos\delta cos\varphi cos\omega + sin\delta sin\varphi \\ cos\gamma_s = \frac{sin\delta - sin\alpha_s sin\varphi}{cos\alpha_s cos\varphi} \end{cases} \quad (4)$$

where φ is the local latitude, positive for north latitude; ω is the solar time angle, the formula is as follows:

$$\omega = \frac{\pi}{12}(ST - 12) \quad (5)$$

where ST is the local time and δ is the angle of solar declination. The formula of δ is as follows:

$$sin\delta = sin\frac{2\pi D}{365}\sin(\frac{2\pi}{360}23.45) \quad (6)$$

where D is the number of days counted from the vernal equinox as day 0, the value of D for the 21st day of each month is calculated as Table 1:

Table 1: The date corresponds to D

January 21	February 21	March 21	April 21	May 21	June 21
306	336	0	31	61	92
July 21	August 21	September 21	October 21	November 21	December 21
122	153	184	214	245	275

The final calculated azimuth and altitude angles are shown in Fig 1.

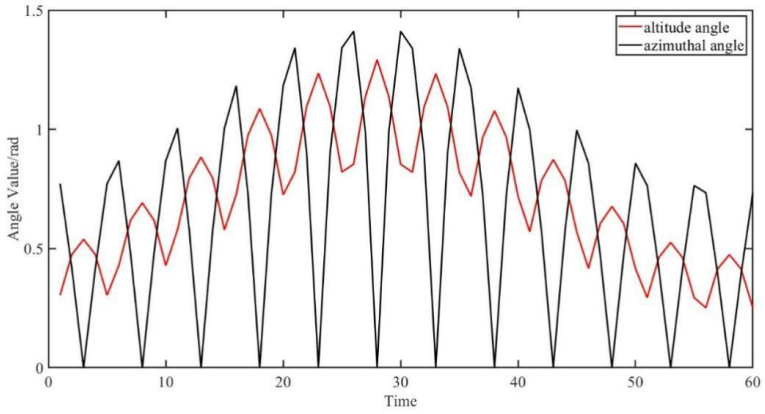

Figure 1: The changes in solar altitude and azimuth

After obtaining the solar azimuth and altitude angle at each moment, the vector of incident light $\vec{\imath}$ at each moment can be calculated. The formula is as follows:

$$\vec{\imath} = (cos\gamma_s cos\alpha_s, cos\alpha_s sin\gamma_s, sin\alpha_s) \quad (7)$$

4. The model of optical efficiency

The optical efficiency has five sub-efficiencies consisting of a constant 0.92 for specular reflectance and an atmospheric transmittance that can be calculated from the following equation:

$$\eta_{at} = 0.99321 - 0.0001176 d_{HR} + 1.97 \times 10^{-8} \times d_{HR}^2 \quad (8)$$

where d_{HR} is the distance from the center of the mirror to the center of the collector.

In summary, the three factors that need to be modeled for discussion are the shadow shading efficiency, the cosine efficiency, and the truncation efficiency.

4.1 Cosine efficiency

It is obtained from the relevant literature[6,7] that the cosine efficiency is the cosine of the angle of incidence of the light ray, so $\eta_{cos} = cos\theta$. θ is the angle of incidence angle, then the cosine efficiency can be found by finding the value.

Establish a planar Cartesian coordinate system centered on the collector, with the ground as the oxy-plane, expanding to a spatial Cartesian coordinate system. The reflected ray vector is determined by the coordinates of the mirror center of the fixed-sun mirror (x, y, z) and the coordinates of the collector $(0,0,h)$, so the vector of reflected ray $\vec{r} = (x, y, z-h)$. And according to the law of reflection:

$$\vec{\imath} + \vec{r} = 2\vec{n}cos\theta \tag{9}$$

Then the mirror normal vector $\vec{n}$ can be obtained.

4.2 Efficiency of shadow occlusion

Based on the relevant literature[8], it can be summarized that the efficiency loss due to shadow shading consists of two main components. The first part is the loss of light due to shading between the heliostat and neighboring heliostats. The second part is due to the absorption tower in the sun under the shadow, and cause in the shadow of the fixed sun mirror can not absorb the sunlight generated by the loss of light.

Firstly, discussed the first part of the loss. Two neighboring mirrors, A and B, establish a mirror coordinate system using the fixed-sun mirror's center as the origin, and the same coordinate system is established on mirror B as shown in Fig 2. Find the conversion formula for the A coordinate system, B coordinate system, and the ground coordinate system. That is, the transformation matrix T:

$$T = \begin{matrix} -sinE_H & -sinA_H cosE_H & cosA_H cosE_H \\ cosE_H & -sinA_H sinE_H & cosA_H sinE_H \\ 0 & cosA_H & sinA_H \end{matrix} \tag{10}$$

A_H is the angle between the mirror surface of the fixed-sun mirror and the ground normal, and is the angle between the normal vector of the mirror surface and the y-axis of the ground coordinate system. The specific conversion process will not be discussed too much here as it has been given in the related literature[9,10]. In conclusion, mirror A is divided into grid points with a step size of 0.01m, and traversing these points will give us a conclusion about whether these points will fall on mirror B. Then the ratio of points falling on mirror B to the total number of points is the loss of shadow masking efficiency. And shadow shading efficiency = 1 - loss of shadow shading efficiency.

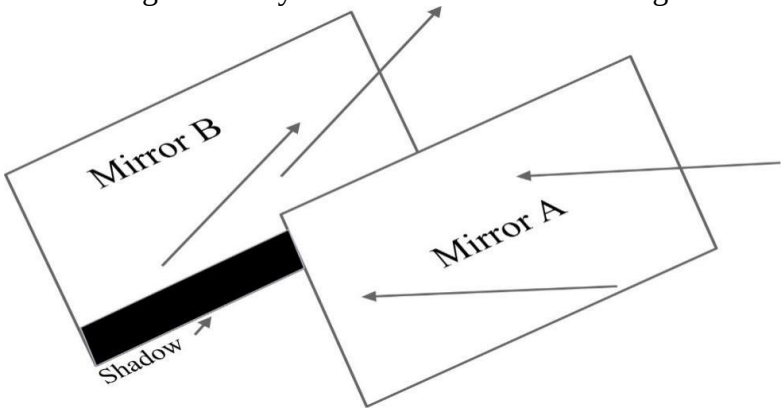

Figure 2: Schematic diagram of shadow light blocking effect

After traversing the program it is obtained that there is no case where occlusion occurs in the front and back mirrors, so the shadow occlusion efficiency is only determined by the second part. The second part is discussed next.

The second part of the loss is determined by the shadowing caused by the absorber tower, then the shaded area is represented and the number of heliostats that are in the shaded area can be found by traversing the coordinates of all heliostats.

Firstly, the representation of the shaded area is discussed. Since the diameter of the absorption tower is much smaller than the diameter of the heliostat field, the absorption tower can be regarded as a thin rod, and according to the relevant literature and mathematical.

$$l = \frac{L}{\frac{\pi}{2} - n(\frac{\pi}{2} - arcsin\alpha_s)} \tag{11}$$

L is the height of the thin rod and n is the atmospheric refractive index, which in this case is taken to be the constant 1.0003. Solve the program to obtain the value of L at 60 moments. And the shaded area can be considered as a rectangle which can be represented by four straight lines:

$$\begin{cases} y = cos\gamma_s x - \frac{3.5}{cos\gamma_s} \\ y = cos\gamma_s x + \frac{3.5}{cos\gamma_s} \\ y = -cos\gamma_s x \\ y = -cos\gamma_s x - \frac{l}{sin\gamma} \end{cases} \tag{12}$$

4.3 Cut-off efficiency

The ray of light formed by the reflection of a mirror is conical. Since the sun's rays are actually conical rays, the conical beam converges and concentrates at the center of the heliostat, and is reflected to form a spot on the collector. Because of the limited size of the collector, this results in part of the spot being truncated, also known as the light overflow phenomenon. Defining the spot boundaries by the fringe rays of the conical rays, the angle of incidence is θ. From the straight line distance between the center of the mirror and the center of the collector, the radius of the circular spot can be found to be r. A simple focusing strategy was used to simply position the reflective spot of the heliostat at the center of the vertical height of the collector. Fig 3 is the Schematic diagram of truncation effect. The truncation efficiency can be expressed as:

$$\eta_{trunc} = \frac{R}{R + 2d_{HR}tan\theta} \tag{13}$$

R is the diameter of the cylindrical collector. Both of the angle of incidence and the distance between the two center positions can be calculated from the previous equations. This equation is then used to solve for the truncation efficiency at each point in time for each fixed-day mirror, which in turn calculates the annual average truncation efficiency.

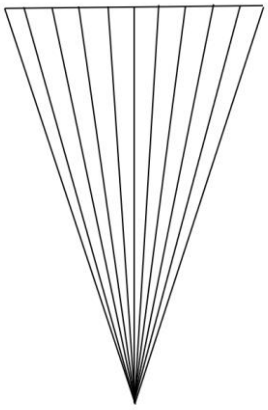

Figure 3: Schematic diagram of truncation effect

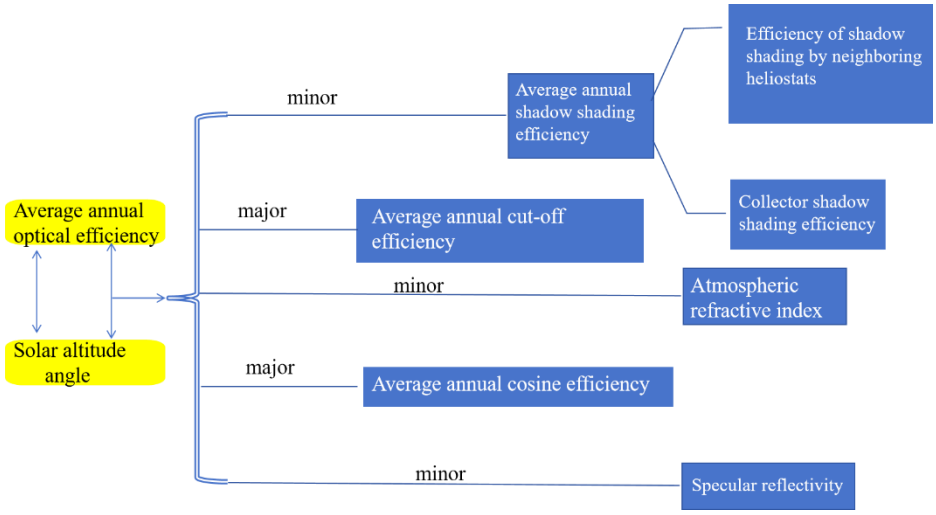

Figure 4: Schematic diagram of optical efficiency composition

Fig 4 is the schematic diagram of optical efficiency composition, which help readers understand composition better.

5. Mirror field arrangement

After establishing the physical model of the mirror field, the optimal arrangement of the mirror field is discussed. In the actual power production, the construction cost of the mirror field is related to the construction complexity of the mirror field, the number of mirrors, the size of the mirrors and other factors[11-13]. Generally speaking, in the case of a certain optical efficiency, the more the number of mirrors, the larger the mirror size, the larger the annual average output thermal power, but the corresponding construction cost will also be larger. Therefore, the thermal power per unit mirror surface area can be used as the target value, and when the thermal power per unit mirror surface area is maximized, it is determined that the mirror field arrangement is optimal at this time.

5.1 Comparison of three types of arrangements

In the construction of actual tower solar thermal power systems, mirror fields are often arranged in four ways, square, circular, Campo, and bionic. According to the relevant literature[14-16], Campo

arrangement and bionic arrangement are not adopted in the actual construction because the construction difficulty and cost of Campo arrangement and bionic arrangement are much larger than their net gain in optical efficiency. This paper also innovates an arrangement, the Dense Circular Arrangement. Optical efficiency and annual average thermal power per mirror area for the three arrangements are discussed next.

It is assumed that a circular heliostat field will be constructed in a circular area centered at 98.5∘ E, 39.4∘ N, 3000 m above sea level, and 350 m radius. Take the center of the circular area as the origin, the east direction as the x-axis positive, the north direction as the y-axis positive, and the upward direction perpendicular to the ground as the z-axis positive to establish a coordinate system, which is called the mirror field coordinate system. The planned height of the absorber tower is 80 m. The collector is a cylindrical light-exposed collector with a height of 8 m and a diameter of 7 m. No heliostat will be installed within 100 m of the absorption tower, leaving open space for the construction of a plant for the installation of power generation, energy storage, control and other equipment. The heliostats are square in shape and have sides between 2 m and 8 m in length. Fixed-sun mirrors can be installed at a height of between 2 m and 6 m. They must be mounted at such a height that the mirror surface does not touch the ground when rotating on a horizontal axis. The distance between the centers of the bases of the adjacent heliostats is required to be more than 5 m more than the width of the mirror due to maintenance and cleaning vehicle traffic[17].

The next section describes the dense circular arrangement in this construction environment. This type of arrangement is arranged from inside to outside according to the circle layer, because it is required that no heliostat is allowed to be placed within 100m of the absorption tower, so the first circle is arranged from 100 m. The question also requires that the distance between the centers of the bases of adjacent heliostats be more than 5 m more than the width of the mirror, the distance between the centers of adjacent mirrors is $\left(\sqrt{S_0}+5\right)m$. S_0 is mirror area. The first mirror is lined up first, and the coordinates of the first mirror are (100, 0) according to the form of polar coordinates. Rearranging the second mirror, the angle increment can be approximated to be $\frac{2\pi}{2\pi\rho}\sqrt{S_0}+5$ since it is small. Similarly after lining up this circle of fixed-sun mirrors, the next circle is lined up in the same increments. And so on until the number of heliostats reaches the required total number n of heliostats. It is verified by the program that this arrangement does not cause shadow blocking between two adjacent heliostats.

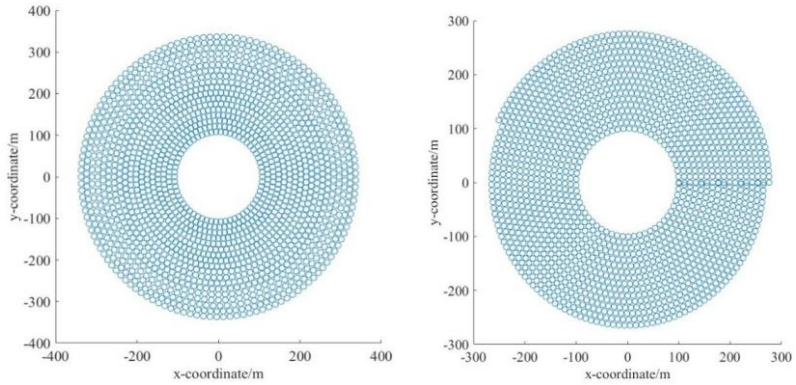

Figure 5: Traditional circular arrangement and dense circular arrangement

In a traditional circular arrangement, 1,745 mirrors can be arranged in the construction environment described above. Setting the size of both day mirrors as 6 m×6 m and the installation height as 4 m, the average annual thermal power output was calculated to be 36.67 MW. And the same arrangement of 1745 mirrors by dense circular arrangement has an average annual thermal

power output of 37.88 MW. It can be seen that the output thermal power per unit mirror area of dense circular arrangement is greater than that of traditional circular arrangement, i.e., the production efficiency is higher. The layout diagrams of the two types of arrangement are shown in Fig 5.

5.2 Optimized and improved dense circular arrangement

The use of modern optimization algorithms can further improve the heliostat mirror field under dense circular arrangement to maximize the thermal power output per unit mirror area. According to the established mathematical model, the installation height of the heliostat mirrors in the heliostat field affects the optical efficiency of the mirrors. According to the results of the optimization algorithm, it is concluded that increasing the height of the heliostat mirrors from the inside to the outside of the heliostat mirror field can effectively increase the optical efficiency of the mirror field. So changing the mounting height of the heliostat mirror in each ring of the mirror field can effectively enhance the average thermal power output per unit area of the mirror. There are a total of 15 circles in the heliostat field, and the installation height is limited to between $2-6m$, so the height of the first circle is taken as 2 m, and then each circle is raised by $\frac{4}{15}m$ in turn. The final calculation gives an average annual thermal power output of 38.81 MW, which is an improvement over the pre-improvement effect.

6. Conclusion

In the end, this paper got the best mirror setup. In this paper, the mathematical model of heliostat mirror field is established by considering the solar ray model, optical efficiency model of heliostat mirror, and geographical factors, so that the average annual output power of the mirror field and the power per unit mirror area can be calculated according to the mirror field arrangement. In this way, the economic benefits of heliostat mirror field can be measured, which can help the related industry personnel to get the optimal mirror field arrangement. However, there are still many problems in this paper, such as the establishment of the mathematical model of the mirror field does not take into account economic, environmental and other factors, the power per unit of mirror area as the only measure of this value. Therefore, a comprehensive evaluation model TOPSIS, fuzzy comprehensive evaluation method should be established to get a more realistic mirror field arrangement.

References

[1] F. Eddhibi, A.B. Ali, M. Ben Amara, M. Balghouthi, A.A. Guizani, A novel mathematical approach for the optical efficiency optimization of solar tower power plant technology, International Journal of Energy Research 46 (2022) 2477-2499.

[2] W.M. Hamanah, A.S. Salem, M.A. Abido, F.A. Al-Sulaiman, A.M. Qwbaiban, T.G. Habetler, Modeling, Implementing, and Evaluating of an Advanced Dual Axis Heliostat Drive System, J. Sol. Energy Eng. Trans.-ASME 144 (2022) 14.

[3] A. Belaid, A. Filali, A. Gama, B. Bezza, T. Arrif, M. Bouakba, Design optimization of a solar tower power plant heliostat field by considering different heliostat shapes, International Journal of Energy Research 44 (2020) 11524-11541.

[4] H.M.A. Hayat, S. Hussain, H.M. Ali, N. Anwar, M.N. Iqbal, Case studies on the effect of two-dimensional heliostat tracking on the performance of domestic scale solar thermal tower, Case Stud. Therm. Eng. 21 (2020) 11.

[5] R. Singhai, H. Sinhmar, N.D. Banker, Effect of Aspect Ratio of Heliostat on Cost of Energy from Solar Power Tower Plants, Arab. J. Sci. Eng. 45 (2020) 877-890.

[6] C. Corsi, M.J. Blanco, V. Grigoriev, J. Pye, Upper limits to the mean annual optical efficiency of solar mono-tower systems, Sol. Energy 236 (2022) 88-99.

[7] J. Wang, L. Duan, Y. Yang, L. Yang, Rapid design of a heliostat field by analytic geometry methods and evaluation of maximum optical efficiency map, Sol. Energy 180 (2019) 456-467.

[8] A.A. Rizvi, D. Yang, A detailed account of calculation of shading and blocking factor of a heliostat field, Renew. Energy 181 (2022) 292-303.

[9] Q.Y. Xie, Z.Q. Guo, D.F. Liu, Z.S. Chen, Z.L. Shen, X.L. Wang, Optimization of heliostat field distribution based on improved Gray Wolf optimization algorithm, Renew. Energy 176 (2021) 447-458.
[10] Q.Y. Xie, Y.X. Xiao, X.L. Wang, D.F. Liu, Z.L. Shen, Heliostat Cluster Control for the Solar Tower Power Plant Based on Leader-Follower Strategy, IEEE Access 7 (2019) 135031-135039.
[11] S.O. Fadlallah, T.N. Anderson, R.J. Nates, Artificial Neural Network-Particle Swarm Optimization (ANN-PSO) Approach for Behaviour Prediction and Structural Optimization of Lightweight Sandwich Composite Heliostats, Arab. J. Sci. Eng. 46 (2021) 12721-12742.
[12] W.D. Huang, L. Yu, P. Hu, An analytical solution for the solar flux density produced by a round focusing heliostat, Renew. Energy 134 (2019) 306-320.
[13] I. Moreno-Cruz, J.C. Castro, O. Alvarez-Brito, H.B. Mota-Nava, G. Ramírez-Zúñiga, J.J. Quiñones-Aguilar, C.A. Arancibia-Bulnes, Development of an Elevation-Fresnel Linked Mini-Heliostat Array, Energies 13 (2020) 19.
[14] K. Lee, I. Lee, Optimization of a heliostat field site in central receiver systems based on analysis of site slope effect, Sol. Energy 193 (2019) 175-183.
[15] E. Leonardi, L. Pisani, I. Les, A.M. Larrayoz, S. Rohani, P. Schöttl, Techno-economic heliostat field optimization: Comparative analysis of different layouts, Sol. Energy 180 (2019) 601-607.
[16] A.A. Rizvi, D. Yang, T.A. Khan, Optimization of biomimetic heliostat field using heuristic optimization algorithms, Knowledge-Based Syst. 258 (2022) 14.
[17] J.G. Wales, A.J. Zolan, A.M. Newman, M.J. Wagner, Optimizing vehicle fleet and assignment for concentrating solar power plant heliostat washing, IISE Trans. 54 (2022) 550-562.